Available online at www.sciencedirect.com

ScienceDirect

IFAC PapersOnline CONFERENCE PAPER ARCHIVE

IFAC PapersOnLine 54-14 (2021) 144–148

# A New Modeling Approach for Stability of Micro/Nano Bubbles

**Mustafa Doğan** * **Ulviya Bunyatova** ** **Onur Ferhanoğlu** ***

* *Istanbul Technical University, Faculty of Electrical-Electronics Engineering, Department of Control and Automation Engineering, 34469, Istanbul, Turkey (e-mail: mustafa.dogan@ gmail.com).*
** *Baskent University, Faculty of Engineering, Department of Biomedical Engineering, Baglica Kampusu, 06790 Ankara, Turkey (e-mail:ubunyatova@baskent.edu.tr)*
*** *Istanbul Technical University, Faculty of Electrical-Electronics Engineering, Department of Electronics and Communications Engineering, 34469, Istanbul, Turkey (e-mail:ferhanoglu@itu.edu.tr)*

**Abstract:**
Microbubbles and nanobubbles have several characteristics that are comparable with millimeter- and centimeter-sized bubbles. These characteristics are their small size, which results in large surface area and high bioactivity, low rising velocity, decreased friction drag, high internal pressure, large gas dissolution capacity, negatively charged surface, and ability to be crushed and form free radicals. Controlling and modeling fundamental properties such as nucleation and of the dynamics of these bubbles is key to successfully exploiting their potential in the growing number of applications such as biomedical diagnosis and therapy, antimicrobial in aquaculture, environment, engineering, stock raising and marine industry. Laser-generated bubble dimensions can be characterized with an optical setup employing a high power continuous wave green laser for bubble generation. In this work, non-resonant, self-excited due to structurally nonlinear properties of the hydrogel, bubble formation was modeled as functions of well-controlled parameters of the colloidal media that is multi-layered and anisotropic, engineered uniquely.



*Keywords:* nano bubbles, anisotropic, colloidal, laser treatment, modeling, pump-probe

## 1. INTRODUCTION

The main objective is to facilitate the growth of long lasting nano / micro bubbles, unlike an immense amount of literary studies that present short-duration bubbles. The longevity of a bubble - along with a trigger mechanism to demolish it at a desired instant - is particularly appealing in a number of applications; one possible application could be a targeted drug delivery scenario, where the drug encapsulating bubble array is exploded at the desired tissue site. Another application is water treatment to cope with wide pollution. Long lasting bubbles encapsulating pollutants can be demolished at pre-allocated waste. While we will focus on reliable generation of long-lasting (more than 72 hours) bubbles and develop a modeling framework, we will also be targeting the following side objectives: i) Characterizing the lifetime not only in still and steady diluted solutions as well as streams to mimic blood flow (as in drug delivery scenario) or water treatment (in the seas and oceans). ii) Demonstrate controlled demolition of the bubbles, once again using pulsed lasers, potentially at different power regimes and wavelengths. iii) Developing micro and macro optical platforms to adapt the bubble generation and demolition to bodily cavity (i.e. vessel) dimensions or water treatment at large scale.

Micro and nano bubbles, MNBs have many applications, e.g. biomedical diagnosis and therapy, the delivery of chemotherapy drugs, aquaculture, environment, engineering, stock raising, microfluidics, sterilization using ozone gas and marine industry Dijkmans et al. (2004); Diop and Taylor (2006); Jang et al. (2019); Khayatzadeh et al. (2017); Lindner (2004); Unger et al. (2001). Usually, MNBs are gas-containing cavities in aqueous solution with unique physical characteristics that differ from macro bubbles. While microbubbles are smaller than macro bubbles with a diameter range of $1\mu m...100\mu m$ Azevedo et al. (2016), these bubbles shrink in the water and then dissolve into it. In contrast, NBs are extremely small gas bubbles that have several unique physical properties that make them very different from normal bubbles. Generally, NBs range is $\ll 1\mu m$ in diameters Azevedo et al. (2016) randomly drift termed as Brownian Motion and with a lower buoyancy can remain suspended in liquids for an extended period of time and have the ability to change the typical characteristics of water as being colloidal. Nanobubbles with $150...200nm$ can survive up to a few weeks or more Meegoda et al. (2018); Azevedo et al. (2016). However, the microbubbles can reach lifetime only up to tens of minutes Angelsky et al. (2017) or exist for a long period of time only under certain energy “feeding” laser regime with 0.3W power. There are more than several models reported elsewhere to explain stabilization mechanism of nano bubbles, but none of them yet succeeded.Despite subsequent studies, there are still controversies over MNBs size and its existence in the solutions under atmospheric conditions. MNBs are generated on the surface of hydrophobic particles FAN et al. (2010). Depending on internal or external factors, the


10.1016/j.ifacol.2021.10.343

formation of MNBs can be induced in several possible ways Oshemkov et al. (2009). Literature shows that the distribution and size of MNBs depend on the system design and various operational conditions. Further literature shows ambiguity in terms of fundamental properties, such as stability of bulk NBs that is not explained properly up to now. Only a few experimental studies deal with the stability and longevity of NBs, with no considerable consensus. The studies have yet to decide whether properties such as separation, stability are following scientific guidelines (classical thermodynamic principles). Although progress has been made and several hypotheses have been proposed explaining the long-term stability of NBs, none of them describe these experimental observations. Our recent studies show that high-power light-matter interaction in a hydrogel nanocomposite structures reveals controllable metallic macro dots formation with the generation of ultra-stable NMBs (up to 3 days due to forced ending intentionally or extended period of time as long as they were kept steady) Litchinitser et al. (2020).

Laser-generated bubble dimensions and dimensional repeatibility can be characterized with an optical setup employing a high power ($\approx 1 - 0.5\,\mathrm{W}$) continuous wave green laser ($532 - 550\,\mathrm{nm}$ wavelength) for bubble generation, and a pilot low power ($\approx 10\,\mathrm{mWs}$) beam that is co-aligned with the high power laser. The scattered light from the bubble can be monitored by one or multiple photo detectors, whose signal strength can be used as an indicator of bubble size. Laser intensity can be altered through focusing with a high numerical aperture lens to eliminate the need for a high power laser.

## 2. MODELING AND CONTROL

In this research, non-resonant, self-excited due to structurally nonlinear properties of the hydrogel, bubble formation will be modeled as functions of well-controlled parameters of the colloidal media that is multi-layered and anisotropic, engineered uniquely. Non-resonant excitation (such that fixed wavelength is not necessary, any frequency can be adjusted) and low-level/short-time laser source requirement are the main differences compare with other experimental techniques in the literature. As proposed significant improvement, refraction index can be defined as a nonlinear function of temperature and other properties of the medium, e.g. conductivity, salinity. To construct this nonlinear model, well-known photo-acoustic governing equations can be good starting point to connect the local temperature gradient and fields inside the layered-anisotropic medium Tang et al. (2010).

Nanobubbles are composed of nucleation, air and shell respectively. Bubbles and their surroundings can be represented multi-layer medium. Note that each layer has their own specific parameters, e.g. heights, $h_1$ and $h_2$, dielectric permittivity, and magnetic permeability, $\epsilon_1, \mu_1$ ,and $\epsilon_2, \mu_2$ respectively. Assume the thickness of the layers is sufficiently small with respect to the wavelength, this type of complex medium behaves on the whole as if it were homogeneous but anisotropic. z-axis perpendicular to layers, propagation along the x-axis, with E directed along the y-axis. Electric field is parallel to the layers -this polarization can be used arbitrarily.

$$\begin{aligned}\bar{\epsilon} &= \frac{h_1\epsilon_1 + h_2\epsilon_2}{h_1 + h_2} \text{ is the mean value of } \epsilon \text{ over a period}\\ \tilde{\mu} = \bar{\mu} &= \frac{h_1 + h_2}{h_1 \,/\, \mu_1 + h_2 \,/\, \mu_2} \text{ is the mean value of } \mu \text{ over a period}\end{aligned} \tag{1}$$

$$\epsilon^e = \bar{\epsilon}\left[1 + \frac{k^2 h_1^2 h_2^2}{12(h_1+h_2)^2}\frac{\bar{\mu}\tilde{\mu}}{\mu_1\mu_2}(n_1^2 - n_2^2)\frac{\epsilon_1 - \epsilon_2}{\bar{\epsilon}}\right], \tag{2}$$

$$\mu^e = \tilde{\mu}\left[1 + \frac{k^2 h_1^2 h_2^2}{12(h_1+h_2)^2}\frac{\bar{\mu}\tilde{\mu}^2}{\mu_1^2\mu_2^2}(n_1^2 - n_2^2)(\mu_1 - \mu_2)\right] \tag{3}$$

where $k = \omega/c$ is the wavenumber, $k_1 = kn_1$, $k_2 = kn_2$ wavenumbers for layer 1 and 2 respectively and $n_1^2 \equiv \epsilon_1\mu_1$, $n_2^2 \equiv \epsilon_2\mu_2$ Brekhovskikh (1960).

Then we can derive the energy density per volume ($W/m^3$) by using relationship between Electric Field (source/control) and propagated power Pozar (2005).

$$p_l(r,t) = \frac{n_1}{4c}\sqrt{\frac{\epsilon^e}{\mu^e}}\,\|\mathbf{E}(r,t)\|^2\,\frac{1}{r} \tag{4}$$

where $n_1$ is refractive index of the first layer, $c$ is the speed of the light, $\mathbf{E}$ is the surface electric field, parallel to the layers, $r$ is the spherical distance to the nucleation, and $\epsilon^e, \mu^e$ effective dielectric permittivity, and magnetic permeability in equations (2)- (3).The anisotropy of the medium, resulting in the growth of the overall refractive index ($n = \sqrt{\mu^e\,\epsilon^e}$) which is the origin of the non-linear dispersion. On the other hand, nonlinear dispersion can cause compression and focusing unlike the linear case.

The time-dependent temperature field $T(r,t)$ where $0 \le r \le L$ around a single nanoparticle, assuming spherical geometry and constant thermal properties, is governed by the spherical linear Fourier equation for heat conduction Wang et al. (2018):

$$\partial_t T(r,t) = \frac{p_l(r,t)}{\rho c_p} + \frac{\kappa}{r^2}\partial_r(r^2\partial_r T(r,t)) \tag{5}$$

where $\kappa$, $\rho$, and $c_p$ are thermal diffusivity, density, and heat capacity of liquid assuming $\kappa\rho\,c_p = 1$ for water, and $p_l(r,t)$ is the deposited power density is explicitly given in (4). Boundary conditions for near insulation at the both ends are given as $\partial_r T(0,t) = \partial_r T(L,t) = 0$ for adiabatic system. We get the following steady state solution for zero time-derivative of temperature,

$$T(r,t) = \frac{A}{r} - Cr\,e^{-\alpha t} + B \tag{6}$$

where $A, B, C$, and $\alpha$ are appropriate real positive constants. After the certain decaying time due to absorption and heat conversion, the control term in equation (6) will vanish exponentially where $C$ is the control parameter. Then the first term will be attenuated by distance linearly. Obviously, temperature and pressure will be stabilized around the equilibrium point. At the beginning, laser light as controlled source can dominate the generation of bubbles and initial excitation. Upon completion of this initialization, source is turned off, then we observed that bubbles stayed steady for long time.

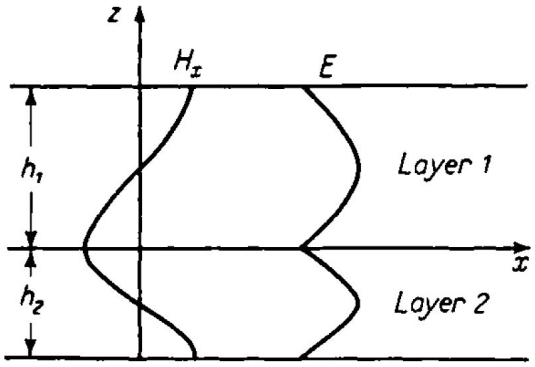


Fig. 1. Finely layered media Brekhovskikh (1960)

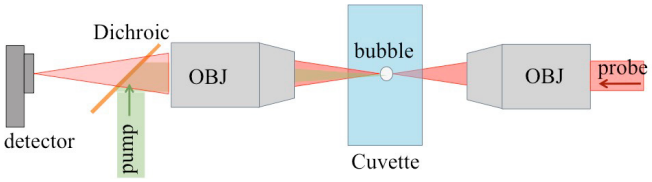


Fig. 2. Bubble pump-probe setup that comprises a pump and a probe beam. The beams having different wavelengths can be isolated via a dichroic filter placed before the detector, adapted from Schaffer et al. (2001).

The life-time of bubbles can be controlled once the model is obtained. In a pre-controlled fashion to collapse the bubbles at the specific time and local spatial coordinates, heat inside the bubble can be increased tacitly by the following method: Self-triggered catalytic decomposition of specific compounds, possibly excited with some enzymes.

Laser-generated bubble dimensions and dimensional repeatability can be characterized with an optical setup employing a high power continuous wave laser or a pulsed laser for bubble generation, and a pilot low power beam that is co-aligned with the high power laser. Both lasers are combined via dichroic filters, and thoroughly align share the same focusing lens, ending up at the same focus. A fluid chamber is typically employed to serve as the medium in which bubbles are created.

The scattered light from the bubble can be monitored by one or multiple photo-detectors, whose signal strength being used as an indicator of bubble size Haering (2010). The measurement in a pump probe setup rely on scattering of laser-induced bubbles for tracking the growth and collapse. The detector collects unscattered light to track bubble dynamics.

The bubble pump-probe setup has been employed in a number of different studies, such as a i) non-toxic probe for measuring functional properties of individual cells Lapotko (2006), and in investigating the mechanisms of laser-induced breakdown in transparent media Schaffer et al. (2001), see e.g. Figure 2.

The bubble pump-probe setup can potentially be integrated with ultrasound transducer(s) Aglyamov et al. (2008) and a camera as complementary techniques to characterize bubble size, as well as its lifetime. While pump-probe provides unprecedented size measurement capability, addition of ultrasound and a camera will potentially be an innovative asset to the best of our knowledge - in bubble characterization) enable tracking of the lifetime of the generated bubbles.

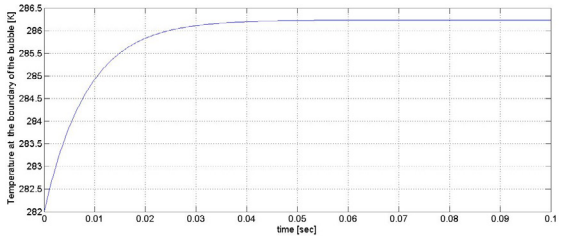


Fig. 3. Temperature around the bubble membrane, $r = 0.1$ mm.

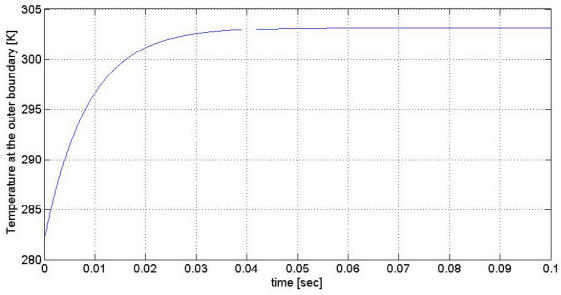


Fig. 4. Temperature around the outer boundary where the laser light embraced at first, $r = 1$ mm.

## 3. SIMULATIONS

| Parameter | Value |
|---|---|
| Height of the first layer, | $h_1 = 1e-3\,m$ |
| Height of the second layer, | $h_2 = 1e-4\,m$ |
| Time step | $\Delta t = 1e-4$ sec |
| Spatial step | $\Delta x = 0.0244 \quad mm$ |
| Relative dielectric permittivity, | $\epsilon_1 = 1.7777, \quad \epsilon_2 = 1$ |
| Relative permeability | $\mu_1, \mu_2 \approx 1$ |
| Refractive index | $n_1^2 = \epsilon_1\mu_1, n_2^2 = \epsilon_2\mu_2$ |
| Wavenumber | $k = 1.1788e+7$ |
| Attenuation constant | $\alpha = 0.0118$ |

Table 1. Parameters of the Layers.

The thermal system (5) without pump-probe setup is tested fully with the simulation program implemented in MATLAB. The PDEs are discretized in the space domain by the finite difference method, to obtain ODEs at each of the nodes. Then, ODEs are solved numerically. The explicit finite difference scheme that requires very small time-steps and easy to implement efficiently, is adapted from Abhyankar et al. (1993). On the other hand, robust numerical stability is succeeded by making the ratio $\Delta t / \Delta x^2 \leq 0.5$ as low as possible. The parameters for the system (5), are listed in Table 1. The parameter set obtained through preliminary experimental trials with characterization measurements.

Obviously, $A \ll B, C$ can be inferred for the parameters in equation (6). Because, the temperature has increasing behavior along time and spatial coordinates , e.g. see Figures 3 and 4. Attenuation constant, $\alpha$ is chosen in compliance with the complex part of refractive index inside the bubble. Steady-state behavior is achieved with choosing the right parameters and setting the source term, namely $p_l(r,t)$, regarding laser power, e.g. see Figures 4 and 5. Heat flow in Figure 5 is complying with adiabatic boundary conditions to be satisfied physically. All boundary conditions among layers are validated with extensive experimental tests.

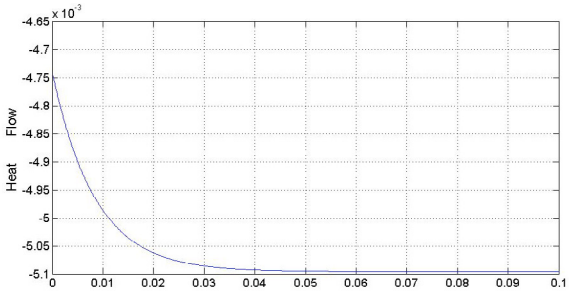


Fig. 5. Laplacian of the temperature or heat flow.

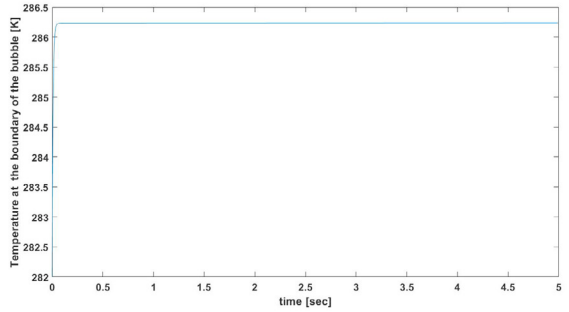


Fig. 6. Temperature around the bubble membrane for long time, $r = 0.1$ mm.

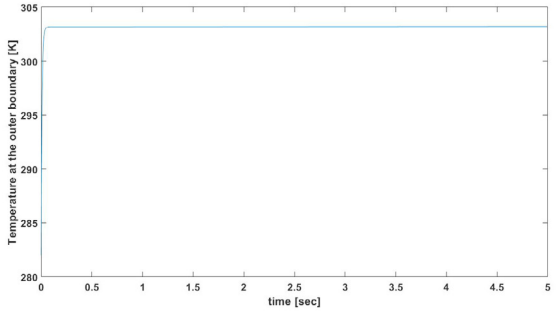


Fig. 7. Temperature around the outer boundary where the laser light embraced at first for long time, $r = 1$ mm.

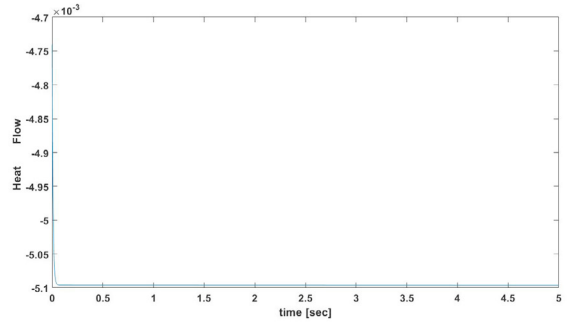


Fig. 8. Laplacian of the temperature or heat flow for long time.

## 4. CONCLUSION

Finally, designed bubbles with long term stability, can give us to control their life-cycle with various novel methods, e.g. self-triggered, self-excited by using the structural nonlinearities and unique synthesis of 3-D hybrid polymer matrices with new techniques based on the advanced model based on interdisciplinary work. Consequently, we obtain the ultra-stable bubbles without external continuous excitation.

In the sense of nonlinear model, our research has important contribution for relating the refractive index to temperature gradient. Thus, we can design the experiment more rigorously. Our simulation results show that the achieved steady state is satisfactory for couple of seconds. In the figures, short time window is preferred to see the details. Furthermore, we are ready to implement the setup for advanced experiments.

## REFERENCES

Abhyankar, N.S., Hall, E. K., I., and Hanagud, S.V. (1993). Chaotic vibrations of beams - Numerical solution of partial differential equations. *ASME Journal of Applied Mechanics*, 60(1), 167–174.

Aglyamov, S.R., Karpiouk, A.B., Bourgeois, F., Ben-Yakar, A., and Emelianov, S.Y. (2008). Ultrasound measurements of cavitation bubble radius for femtosecond laser-induced breakdown in water. *Opt. Lett.*, 33(12), 1357–1359. doi: 10.1364/OL.33.001357.

Angelsky, O.V., Bekshaev, A.Y., Maksimyak, P.P., Maksimyak, A.P., Hanson, S.G., and Kontush, S.M. (2017). Controllable generation and manipulation of micro-bubbles in water with absorptive colloid particles by cw laser radiation. *Opt. Express*, 25(5), 5232–5243.

Azevedo, A., Etchepare, R., Calgaroto, S., and Rubio, J. (2016). Aqueous dispersions of nanobubbles: Generation, properties and features. *Minerals Engineering*, 94, 29 – 37. doi: https://doi.org/10.1016/j.mineng.2016.05.001.

Brekhovskikh, L.M. (1960). *Waves in layered media / by Leonid M. Brekhovskikh ; translated from the Russian by David Lieberman ; translation edited by Robert T. Beyer*. Academic Press New York.

Dijkmans, P., Juffermans, L., Musters, R., van Wamel, A., ten Cate, F., van Gilst, W., Visser, C., de Jong, N., and Kamp, O. (2004). Microbubbles and ultrasound: from diagnosis to therapy. *European Journal of Echocardiography*, 5(4), 245–246. doi:10.1016/j.euje.2004.02.001. URL `https://doi.org/10.1016/j.euje.2004.02.001`.

Diop, M. and Taylor, R. (2006). Soft Trapping and Manipulation of Cells Using a Disposable Nanoliter Biochamber. *Biophysical Journal*, 90(10), 3813–3822. doi: 10.1529/biophysj.105.075614.

FAN, M., TAO, D., HONAKER, R., and LUO, Z. (2010). Nanobubble generation and its application in froth flotation (part i): nanobubble generation and its effects on properties of microbubble and millimeter scale bubble solutions. *Mining Science and Technology (China)*, 20(1), 1 – 19. doi: https://doi.org/10.1016/S1674-5264(09)60154-X.

Haering, S.W. (2010). *Nanoparticle Mediated Photodistruption*. Master's thesis, The University of Texas at Austin, THE UNIVERSITY OF TEXAS AT AUSTIN. An optional note.

Jang, D., Lee, J., Song, H., Park, H., Hong, J., and Chung, S.K. (2019). Optothermally pulsating microbubble-mediated micro-energy harvesting in underwater medium. *Review of Scientific Instruments*, 90(9), 095004. doi:10.1063/1.5097298. URL `https://doi.org/10.1063/1.5097298`.

Khayatzadeh, R., Çivitci, F., and Ferhanoğlu, O. (2017). Optimization of piezo-fiber scanning architecture for low voltage/high displacement operation. *Sensors*

*and Actuators A: Physical*, 255, 21 – 27. doi: https://doi.org/10.1016/j.sna.2016.12.025.

Lapotko, D.O. (2006). Laser-induced bubbles in living cells. *Lasers in Surgery and Medicine*, 38(3), 240–248. doi: https://doi.org/10.1002/lsm.20284.

Lindner, J.R. (2004). Microbubbles in medical imaging: current applications and future directions. *Nature reviews. Drug discovery*, 3(6), 527—532. doi:10.1038/nrd1417. URL https://doi.org/10.1038/nrd1417.

Litchinitser, N.M., Sun, J., Pires, D.G., Bunyatova, U., Walasik, W., and Li, W. (2020). Light-matter interactions in engineered turbid media. In *OPTICS and PHOTONICS International Congress 2020*.

Meegoda, J.N., Aluthgun Hewage, S., and Batagoda, J.H. (2018). Stability of nanobubbles. *Environmental Engineering Science*, 35(11), 1216–1227. doi:10.1089/ees.2018.0203. URL https://doi.org/10.1089/ees.2018.0203.

Oshemkov, S.V., Dvorkin, L.P., and Dmitriev, V.Y. (2009). Trapping and manipulating gas bubbles in water with ultrashort laser pulses at a high repetition rate. *Technical Physics Letters*, 35(3), 282–285. doi:10.1134/S1063785009030250.

Pozar, D.M. (2005). *Microwave engineering; 3rd ed.* Wiley, Hoboken, NJ. URL https://cds.cern.ch/record/882338.

Schaffer, C.B., Brodeur, A., and Mazur, E. (2001). Laser-induced breakdown and damage in bulk transparent materials induced by tightly focused femtosecond laser pulses. *Measurement Science and Technology*, 12(11), 1784–1794. doi:10.1088/0957-0233/12/11/305. URL https://doi.org/10.1088/0957-0233/12/11/305.

Tang, M.X., Elson, D.S., Li, R., Dunsby, C., and Eckersley, R.J. (2010). Photoacoustics, thermoacoustics, and acousto-optics for biomedical imaging. *Proceedings of the Institution of Mechanical Engineers, Part H: Journal of Engineering in Medicine*, 224(2), 291–306. doi:10.1243/09544119JEIM598. URL https://doi.org/10.1243/09544119JEIM598. PMID: 20349820.

Unger, E.C., Hersh, E., Vannan, M., Matsunaga, T.O., and McCreery, T. (2001). Local drug and gene delivery through microbubbles. *Progress in Cardiovascular Diseases*, 44(1), 45 – 54. doi:https://doi.org/10.1053/pcad.2001.26443. Contrast Echocardiography.

Wang, Y., Zaytsev, M.E., Lajoinie, G., The, H.L., Eijkel, J.C.T., van den Berg, A., Versluis, M., Weckhuysen, B.M., Zhang, X., Zandvliet, H.J.W., and Lohse, D. (2018). Giant and explosive plasmonic bubbles by delayed nucleation. *Proceedings of the National Academy of Sciences*, 115(30), 7676–7681. doi:10.1073/pnas.1805912115. URL https://www.pnas.org/content/115/30/7676.